

# Distributed Repetitive Learning Control for Cooperative Cadence Tracking in Functional Electrical Stimulation Cycling

Victor H. Duenas<sup>1</sup>, Christian A. Cousin, Courtney Rouse<sup>2</sup>, Emily J. Fox, and Warren E. Dixon<sup>3</sup>

**Abstract**—Closed-loop control of functional electrical stimulation coupled with motorized assistance to induce cycling is a rehabilitative strategy that can improve the mobility of people with neurological conditions (NCs). However, robust control methods, which are currently pervasive in the cycling literature, have limited effectiveness due to the use of high stimulation intensity leading to accelerated fatigue during cycling protocols. This paper examines the design of a distributed repetitive learning controller (RLC) that commands an independent learning feedforward term to each of the six stimulated lower-limb muscle groups and an electric motor during the tracking of a periodic cadence trajectory. The switched controller activates lower limb muscles during kinematic efficient regions of the crank cycle and provides motorized assistance only when most needed (i.e., during the portions of the crank cycle where muscles evoke a low torque output). The controller exploits the periodicity of the desired cadence trajectory to learn from previous control inputs for each muscle group and electric motor. A Lyapunov-based stability analysis guarantees asymptotic tracking via an invariance-like corollary for nonsmooth systems. The switched distributed RLC was evaluated in experiments with seven able-bodied individuals and five participants with NCs. A mean root-mean-squared cadence error of  $3.58 \pm 0.43$  revolutions per minute (RPM) ( $0.07 \pm 7.35\%$  average error) and  $4.26 \pm 0.84$  RPM ( $0.1 \pm 8.99\%$  average error) was obtained for the healthy and neurologically impaired populations, respectively.

**Index Terms**—Distributed control, functional electrical stimulation (FES), FES-cycling, repetitive learning control (RLC).

## I. INTRODUCTION

NEUROLOGICAL conditions (NCs) that result in movement disorders greatly affect a person's

Manuscript received January 29, 2018; revised September 27, 2018; accepted November 13, 2018. Date of publication December 10, 2018; date of current version January 21, 2020. This work was supported by the National Science Foundation under Award 1762829. Any opinions, findings and conclusions or recommendations expressed in this material are those of the author(s) and do not necessarily reflect the views of the sponsoring agency. This paper was recommended by Associate Editor Y. Pan. (*Corresponding author: Victor H. Duenas.*)

V. H. Duenas, C. A. Cousin, C. Rouse, and W. E. Dixon are with the Department of Mechanical and Aerospace Engineering, University of Florida, Gainesville, FL 32611 USA (e-mail: vhdunas@ufl.edu; ccousin@ufl.edu; courtneyrouse@ufl.edu; wdixon@ufl.edu).

E. J. Fox is with the Brooks Rehabilitation Motion Analysis Center, Jacksonville, FL 32216 USA, and also with the Department of Physical Therapy, University of Florida, Gainesville, FL 32610 USA (e-mail: emily.fox@brooksrehab.org).

Color versions of one or more of the figures in this paper are available online at <http://ieeexplore.ieee.org>.

Digital Object Identifier 10.1109/TCYB.2018.2882755

independence and mobility. Rehabilitation technologies aim to improve the motor function using a combination of robotic devices and artificial control to activate muscles related to a specific exercise. Functional electrical stimulation (FES) is a common technology used to elicit muscle contractions to achieve a motor task. Closed-loop FES has been implemented to assist upper-limb tasks [1]–[3], leg tracking experiments [4]–[6], human locomotion via exoskeletons and neuroprostheses [7]–[9], and lower-limb cycling with and without motorized assistance [10]–[14]. FES applied to lower-limb muscles has allowed individuals with spinal cord injury (SCI) to stand and step for short distances, which has improved their sitting balance and posture [15]. Lower-limb FES control generates muscle contractions that induce exercise-related physiological changes and exploit therapeutic benefits compared to pure ambulation with orthoses [15]. Active lower-limb cycling with FES significantly improved the walking ability of stroke participants versus active cycling without FES [16]. Additionally, improvements in postural control and muscle strength after lower-limb FES cycling have been reported for stroke participants [16]. Thus, FES induced cycling has been suggested as a rehabilitation strategy for people with NCs to improve motor skills due to its simplicity, availability, and low risk of injury (e.g., compared to fall risks in locomotion).

Robotic devices have been used to assist neurologically impaired individuals in completing repetitive movements and to quantify kinematic variables to assess the level of motor recovery during clinical studies [17], [18]. Repetition of a movement pattern contributes to motor learning and rehabilitation [17]. Adaptive reorganization of the human motor system after a neurological lesion can be enhanced by activity and task-specific practice [19]. Furthermore, motor learning is promoted primarily during tasks where robotic assistance is provided only as needed to encourage active engagement, if possible, of the user [18], [20]. Hence, the design of a cycling protocol that delivers high intensity repetitive exercise and exploits the benefits of FES is desired. Additionally, motorized assistance can aid in obtaining repeatable exercise by only assisting the electrically stimulated lower-limb muscles as needed.

Learning control methods, such as iterative learning control (ILC) and repetitive learning control (RLC),<sup>1</sup> improve

<sup>1</sup>The acronym RLC is used interchangeably in the introduction of this paper to refer to repetitive learning control (control methodology) and to the designed distributed repetitive learning controller.

the tracking performance of repetitive or periodic processes by utilizing control inputs from previous cycles, iterations, or periods [21]–[23]. The use of learning control does not require an explicit mathematical model of the uncertainties in the system; instead, the control strategy exploits the repeated or periodic motion to learn the uncertainties. Rehabilitation tasks such as cycling are repetitive/periodic naturally; hence, ILC and RLC are attractive methods to adaptively adjust to the person’s unique attributes. Compared to adaptive control, ILC/RLC methods do not require the uncertainty in the system to be linearly parameterizable. This relaxation on the structure of the uncertainty is beneficial given the lack of an exact model in applications that involve human–machine interaction, especially for participants with NCs. ILC and RLC controllers have been synthesized for finite interval tasks with states resetting after each trial [21], [24] and for continuous operation in the time horizon without resetting [25], [26], respectively. In [27], an integral of a kernel multiplied by an influence function estimates a nonlinear repetitive disturbance function; the resulting learning algorithm ensures asymptotic convergence. A saturated learning-based feedforward term was developed in [25] to leverage the periodic nature of the desired trajectory for the control of robot manipulators. An ILC method was developed in [28] to learn from nonidentical tracking tasks. In [26], a fully saturated learning law and an iterative learning formulation to prove convergence of the states were developed.

ILC and RLC methods have been previously implemented in rehabilitation settings with FES. In results such as [24], [29], and [30], the use of ILC with FES has been investigated during planar and unconstrained upper arm tasks for clinical rehabilitation in stroke and multiple sclerosis (MS) populations. However, most of the developed ILC controllers required preliminary model identification procedures, the dynamics were linearized, and limited information was given regarding the switching muscle dynamics. In [31], ILC was implemented for foot trajectory tracking during swing phase in gait using a drop foot neuroprosthesis. A brain–computer interface with FES was developed for upper limb motor rehabilitation using ILC in [32]. Repetitive control was examined in [33] for tremor suppression at the wrist by regulating flexor/extensor muscles.

More recently, a distributed or decentralized learning approach has been developed in the fields of multiagent systems, network control, and large-scale systems. The purpose of distributed control is to use local feedback to generate control actions for the subsystems, thus yielding a flexible framework to obtain a desired global behavior for the overall system. In [34], a distributed ILC approach was realized for trajectory tracking of a group of quadrotors, where each vehicle learns from its own and its neighbor’s previous inputs during past repetitions. Consensus-based learning control was designed to learn periodic uncertainties where an auxiliary control is designed for each follower agent to track the leader in [35]. A distributed adaptive iterative learning technique was implemented for consensus tracking for a class of nonlinear multiagent systems in [36]. In [37], a multiagent formation problem is studied with switching topologies utilizing a distributed algorithm where agents learn to execute a cooperative task via repetition. This paper leverages the idea of distributed

repetitive learning to investigate FES-cycling since the activation of multiple individual muscles is required to achieve a coordinated lower-limb behavior.

Switching across lower-limb muscles is required to achieve metabolic efficiency and smooth coordination during FES-cycling. In [10] and [38], an electric motor provides assistance during regions of the crank cycle where electrical stimulation is less effective at producing torque. Thus, the assist as needed paradigm is applied to the control of the electric motor, while lower-limb muscles are activated via FES. Switching between muscles and an electric motor makes the overall system a switched system. The periodic nature of cycling tasks thus motivates the use of learning control; however, a switched system stability analysis is required.

In this paper, a switched controller with distributed RLC (i.e., an independent learning feedforward input is designed for each actuator) is developed to achieve cadence tracking through the cooperation of six lower-limb muscles and an electric motor mounted to a stationary recumbent cycle. The distributed feedforward learning terms compensate for the periodic dynamics based on the desired cadence tracking trajectory. The switched controller is designed using a nonlinear cycle-rider dynamic model, and it is implemented without the requirement of any identification procedure despite the parametric uncertainty present in the system. The robust feedback terms aid in the rejection of disturbances present in the cycle and in the lower-limbs of the rider (i.e., the non-periodic dynamics). The motivation in this paper is to design a feedforward controller to reduce the influence of high-gain and high-frequency feedback, which leads to accelerated muscle fatigue during muscle stimulation, and better cope with the time periodicity of the cadence tracking. Due to the construction of a filtered tracking error, the distributed RLC affects both cadence and position tracking. Global asymptotic tracking is achieved via a Lyapunov-based stability analysis using a common Lyapunov function that accounts for the periodicity of the system and by invoking a corollary to the LaSalle–Yoshizawa theorem for nonsmooth systems [39, Corollary 2]. Experimental results are reported for seven able-bodied individuals and five participants with different NCs during a 3-min cycling protocol.

## II. NOTATION

Throughout this paper,  $\mathbb{R}^p$  denotes the  $p$ -dimensional Euclidean space,  $\mathbb{R}$  denotes the set of real numbers,  $\mathbb{R}_{>0}$  denotes the set of strictly positive real numbers,  $\mathbb{R}_{\geq t_0}$  denotes the set of real numbers greater than or equal to  $t_0$ ,  $t_0 \in \mathbb{R}$  is the initial time, and  $\mathbb{N}$  denotes the set of all natural numbers. The subscript  $m$  is employed to denote a property, constant, signal, or input related to the muscle groups, while the subscript  $e$  denotes a constant, signal, or input related to the electric motor. The set of crank angles is denoted as  $\mathcal{Q} \subseteq \mathbb{R}$ . The subsets  $\mathcal{Q}_m \subset \mathcal{Q}$  and  $\mathcal{Q}_e \subset \mathcal{Q}$  denote the sets of crank angles where the muscle groups and the electric motor are activated, respectively. The muscle set  $\mathcal{M} \triangleq \{\text{RQuad}, \text{RHam}, \text{RGlute}, \text{LQuad}, \text{LHam}, \text{LGlute}\}$  contains the right ( $R$ ) and left ( $L$ ) quadriceps femoris (Quad),

hamstrings (Ham), and gluteal (Glute) muscle groups, respectively. The set  $\mathcal{N} \triangleq \{1, 2, \dots, N\} \subset \mathbb{N}$  is used to denote the finite set of all possible switching indices, where  $N \in \mathbb{R}_{>0}$  is the total number of subsystems consisting of the activation of a combination of the muscle groups and the electric motor. The actuator set  $\mathcal{A} \triangleq \{\mathcal{M}, \text{Motor}\}$  contains the muscle groups and electric motor. Unless otherwise specified, all the mathematical quantities are assumed to be time-varying, but the functional dependencies are omitted throughout, unless they add clarity.

### III. CYCLE-RIDER DYNAMIC MODEL WITH SWITCHED INPUTS

The stationary cycle-rider system is modeled as a single degree-of-freedom system with the following dynamics [11]:

$$\begin{aligned} M(q)\ddot{q} + V(q, \dot{q})\dot{q} + G(q) + P(q, \dot{q}) + c_d\dot{q} + d(t) \\ = \tau_a(q, \dot{q}, t) + \tau_e(t) \end{aligned} \quad (1)$$

where  $q : \mathbb{R}_{\geq t_0} \rightarrow \mathcal{Q}$  denotes the positive clockwise measurable crank angle;  $M : \mathcal{Q} \rightarrow \mathbb{R}_{>0}$  denotes the combined inertial effects of the rider and the cycle;  $V : \mathcal{Q} \times \mathbb{R} \rightarrow \mathbb{R}$  and  $G : \mathcal{Q} \rightarrow \mathbb{R}$  denote the centripetal-Coriolis and gravitational effects, respectively;  $P : \mathcal{Q} \times \mathbb{R} \rightarrow \mathbb{R}$  denotes the effects of passive viscoelastic tissue forces in the rider's joints;  $c_d \in \mathbb{R}_{>0}$  denotes the viscous damping parameter in the cycle; and  $d : \mathbb{R}_{\geq t_0} \rightarrow \mathbb{R}$  denotes the disturbances applied by the rider (e.g., muscle spasms, etc.) and any other unmodeled effects in the system. The torque applied about the cycle crank axis by the electric motor  $\tau_e : \mathbb{R}_{\geq t_0} \rightarrow \mathbb{R}$  is denoted as

$$\tau_e(t) \triangleq B_e u_e(t) \quad (2)$$

where  $B_e \in \mathbb{R}_{>0}$  is a positive torque constant and satisfies  $B_e \geq c_e$ , where  $c_e \in \mathbb{R}_{>0}$  is a known constant, and  $u_e : \mathbb{R}_{\geq t_0} \rightarrow \mathbb{R}$  is the motor current control input. The net active torque produced by the lower-limb muscle contractions denoted by  $\tau_a : \mathcal{Q} \times \mathbb{R} \times \mathbb{R}_{\geq t_0} \rightarrow \mathbb{R}$  is defined as

$$\tau_a(q, \dot{q}, t) \triangleq \sum_{m \in \mathcal{M}} B_m(q, \dot{q}) u_m(t) \quad (3)$$

where  $B_m : \mathcal{Q} \times \mathbb{R} \rightarrow \mathbb{R}$  represents the uncertain control effectiveness of the involved muscle groups and  $u_m : \mathbb{R}_{\geq t_0} \rightarrow \mathbb{R}$  represents the stimulation intensity applied to each muscle group. The unknown control effectiveness for each muscle group is nonzero and depends on the relationship between the stimulation intensity and the evoked force, and the torque transfer relationship between a muscle's resultant torque about a joint to torque about the crank axis [11].

The stimulation intensity  $u_m$  is applied to each muscle group in regions of the crank cycle where the torque transfer ratios are above a predefined threshold. The switching control design yields an autonomous, state-dependent, and switched control system. The portion of the crank cycle over which a particular muscle group is stimulated is denoted by  $\mathcal{Q}_m \subset \mathcal{Q}, \forall m \in \mathcal{M}$ , where the muscle groups are activated such that  $\mathcal{Q}_M \triangleq \bigcup_{m \in \mathcal{M}} \mathcal{Q}_m$  [11]. The portion of the crank cycle over which the electric motor is switched on is denoted as  $\mathcal{Q}_e \subset \mathcal{Q}$  such that  $\mathcal{Q}_e \triangleq \mathcal{Q} \setminus \mathcal{Q}_M$  (i.e., when no muscle group is stimulated,

the electric motor is active). Based on the system's state, a piecewise constant switching signal can be developed for each muscle group,  $\sigma_m \in \{0, 1\}, \forall m \in \mathcal{M}$  and for the electric motor,  $\sigma_e \in \{0, 1\}$  as

$$\sigma_m(q) \triangleq \begin{cases} 1 & \text{if } q \in \mathcal{Q}_m \\ 0 & \text{if } q \notin \mathcal{Q}_m \end{cases}, \quad \sigma_e(q) \triangleq \begin{cases} 1 & \text{if } q \in \mathcal{Q}_e \\ 0 & \text{if } q \notin \mathcal{Q}_e. \end{cases} \quad (4)$$

Using (4), the stimulation input to the muscle groups and the motor input can be defined as

$$u_m(t) \triangleq k_m \sigma_m(q) (v(t) + \hat{W}_{d,m}(t)) \quad (5)$$

$$u_e(t) \triangleq k_e \sigma_e(q) (v(t) + \hat{W}_{d,e}(t)) \quad (6)$$

respectively, where  $k_m, k_e \in \mathbb{R}_{>0}, \forall m \in \mathcal{M}$  are positive, constant control gains,  $v : \mathbb{R}_{\geq t_0} \rightarrow \mathbb{R}$  is a subsequently designed control input, and  $\hat{W}_{d,m}, \hat{W}_{d,e} : \mathbb{R}_{\geq t_0} \rightarrow \mathbb{R}, \forall m \in \mathcal{M}$  are the RLC laws designed for each muscle and the electric motor, respectively. Substituting (2), (3), (5), and (6) into (1) and rearranging terms yield

$$M(q)\ddot{q} + V(q, \dot{q})\dot{q} + G(q) + P(q, \dot{q}) + c_d\dot{q} + d = B_\sigma (v + \hat{W}_d) \quad (7)$$

where  $B_\sigma \in \mathbb{R}_{\geq 0}$  is a lumped, switched control effectiveness term defined as

$$B_\sigma(q, \dot{q}) \triangleq \sum_{m \in \mathcal{M}} B_m(q, \dot{q}) k_m \sigma_m(q) + B_e k_e \sigma_e(q) \quad (8)$$

and  $\hat{W}_d : \mathbb{R}_{\geq t_0} \rightarrow \mathbb{R}$  is the lumped feedforward learning term. The subscript  $\sigma \in \mathcal{N}$  indicates the index of  $B_\sigma$ , which switches according to the crank position. The known sequence of switching states, which are the limit points of  $\mathcal{Q}_m, \forall m \in \mathcal{M}$ , is defined as  $\{q_n\}, n \in \{0, 1, 2, \dots\}$ , and the corresponding sequence of unknown switching times  $\{t_n\}$  is defined such that each  $t_n$  denotes the instant when  $q$  reaches the corresponding switching state  $q_n$ . The switching signal  $\sigma$  is assumed to be continuous from the right [i.e.,  $\sigma(q) = \lim_{q \rightarrow q_n^+} \sigma(q)$ ] and designed to produce forward pedaling using the state. The following assumption and properties of the switched system in (7) will be exploited in the subsequent control design and stability analysis.

*Assumption 1:* The disturbance term  $d$  is bounded as  $|d| \leq \xi_d$ , where  $\xi_d \in \mathbb{R}_{>0}$  is a known constant.

*Property 1:*  $c_m \leq M \leq c_M$ , where  $c_m, c_M \in \mathbb{R}_{>0}$  are known constants [40].

*Property 2:*  $|V| \leq c_V |\dot{q}|$ , where  $c_V \in \mathbb{R}_{>0}$  is a known constant [40].

*Property 3:*  $|G| \leq c_G$ , where  $c_G \in \mathbb{R}_{>0}$  is a known constant [40].

*Property 4:*  $|P| \leq c_{P1} + c_{P2} |\dot{q}|$ , where  $c_{P1}, c_{P2} \in \mathbb{R}_{>0}$  are known constants [11].

*Property 5:*  $(1/2)\dot{M} - V = 0$  by skew symmetry [40].

*Property 6:* The lumped switching control effectiveness is bounded as  $c_b \leq B_\sigma \leq c_B, \forall \sigma \in \mathcal{N}$ , where  $c_b, c_B \in \mathbb{R}_{>0}$  are known constants.

#### IV. CONTROL DEVELOPMENT

The objective is to design a controller to track a desired crank cadence. A measurable auxiliary tracking error, denoted by  $e_1 : \mathbb{R}_{\geq t_0} \rightarrow \mathbb{R}$  is defined as<sup>2</sup>

$$e_1 \triangleq \int_{t_0}^t (q_d(\varphi) - q(\varphi)) d\varphi \quad (9)$$

where  $q_d : \mathbb{R}_{\geq t_0} \rightarrow \mathbb{R}$  denotes the desired crank position and its first two time derivatives are bounded such that  $|\dot{q}_d(t)| \leq \xi_1$  and  $|\ddot{q}_d(t)| \leq \xi_2$ , where  $\xi_1, \xi_2 \in \mathbb{R}_{>0}$  are known positive constants.

*Remark 1:* The desired crank trajectory is periodic in the sense that  $q_d(t) = q_d(t - T)$ ,  $\dot{q}_d(t) = \dot{q}_d(t - T)$ ,  $\ddot{q}_d(t) = \ddot{q}_d(t - T)$  with known period  $T$ .

To facilitate the subsequent control development, filtered tracking errors  $e_2 : \mathbb{R}_{\geq t_0} \rightarrow \mathbb{R}$  and  $r : \mathbb{R}_{\geq t_0} \rightarrow \mathbb{R}$  are defined as

$$e_2 \triangleq \dot{e}_1 + \alpha_1 e_1 \quad (10)$$

$$r \triangleq \dot{e}_2 + \alpha_2 e_2 \quad (11)$$

where  $\alpha_1, \alpha_2 \in \mathbb{R}_{>0}$  are positive, constant control gains. Taking the time derivative of (11) and premultiplying by  $M$ , substituting for (7), using the second time derivative of (10), and then performing some algebraic manipulation yield

$$M\dot{r} = -Vr + W_d + \chi + N_d - B_\sigma(v + \hat{W}_d) - e_2 \quad (12)$$

where the auxiliary signals  $W_d : \mathbb{R}_{\geq t_0} \rightarrow \mathbb{R}$ ,  $\chi : \mathbb{R}_{\geq t_0} \rightarrow \mathbb{R}$ , and  $N_d : \mathbb{R}_{\geq t_0} \rightarrow \mathbb{R}$  are defined as

$$\begin{aligned} W_d &\triangleq \sum_{i \in \mathcal{A}} W_{d,i} \quad (13) \\ &= \sum_{i \in \mathcal{A}} (M_i(q_d)\ddot{q}_d + V_i(q_d, \dot{q}_d)\dot{q}_d + G_i(q_d)) \end{aligned}$$

$$\begin{aligned} \chi &\triangleq M(q)(\ddot{q}_d + (\alpha_1 + \alpha_2)\dot{e}_2) + V(q, \dot{q}) \\ &\quad \times (\dot{q}_d - \alpha_1^2 e_1 + (\alpha_1 + \alpha_2)e_2) + G(q) + P(q, \dot{q}) + c_d \dot{q} \\ &\quad - W_d - N_d + e_2 \quad (14) \end{aligned}$$

$$N_d \triangleq c_{P1} + (c_{P2} + c_d)\dot{q}_d + d \quad (15)$$

for  $i \in \mathcal{A}$ . The auxiliary signal in (15) can be upper bounded as

$$N_d \leq \Theta \quad (16)$$

where  $\Theta \in \mathbb{R}_{>0}$  is a known positive constant. By using Properties 1–5, (10), and (11), the mean value theorem can be used to develop an upper bound for (14) as

$$\chi \leq \rho(\|z\|)\|z\| \quad (17)$$

where  $z : \mathbb{R}_{\geq t_0} \rightarrow \mathbb{R}^3$  is a composite vector of error signals defined as

$$z \triangleq [e_1 \ e_2 \ r]^T \quad (18)$$

and  $\rho(\cdot) \in \mathbb{R}$  is a known positive, radially unbounded, and nondecreasing function. Based on (13) and the explicit boundedness of the periodic desired trajectory

$$\|W_d(t)\| \leq \beta_r \quad (19)$$

where  $\beta_r \in \mathbb{R}$  is a known positive bounding constant. Given the cadence open-loop error system in (12), the control input is designed as

$$v \triangleq k_1 r + \left( k_2 + k_3 \rho(\|z\|)\|z\| + k_4 \|\hat{W}_d\| \right) \text{sgn}(r) \quad (20)$$

where  $k_1, k_2, k_3, k_4 \in \mathbb{R}_{>0}$  are selectable positive gain constants,  $\text{sgn}(\cdot) : \mathbb{R} \rightarrow [-1, 1]$  is the signum function, and  $\hat{W}_d : \mathbb{R}_{\geq t_0} \rightarrow \mathbb{R}$  is the distributed RLC law designed as

$$\hat{W}_d(t) \triangleq \sum_{i \in \mathcal{A}} \hat{W}_{d,i}(t) = \sum_{m \in \mathcal{M}} \hat{W}_{d,m} + \hat{W}_{d,e} \quad (21)$$

$$\hat{W}_{d,m} \triangleq \sigma_m \left( \text{sat}_{\beta_m}(\hat{W}_{d,m}(t - T)) + k_{L,m} r \right) \quad (22)$$

$$\hat{W}_{d,e} \triangleq \sigma_e \left( \text{sat}_{\beta_e}(\hat{W}_{d,e}(t - T)) + k_{L,e} r \right) \quad (23)$$

where  $k_{L,i} \in \mathbb{R}_{>0}$ ,  $\forall i \in \mathcal{A}$  are learning control gains, and  $\text{sat}_{\beta_i}(\cdot)$  is defined as

$$\text{sat}_{\beta_i}(\Xi_i) \triangleq \begin{cases} \Xi_i & \text{for } |\Xi_i| \leq \beta_i \\ \text{sgn}(\Xi_i)\beta_i & \text{for } |\Xi_i| > \beta_i \end{cases}, \quad \forall i \in \mathcal{A}.$$

The closed-loop error system is obtained by substituting (20) into (12) which yields

$$\begin{aligned} M\dot{r} &= -Vr + \chi + N_d + \tilde{W}_d + \hat{W}_d - e_2 - B_\sigma \\ &\quad \times \left( \hat{W}_d + k_1 r + \left( k_2 + k_3 \rho(\|z\|)\|z\| + k_4 \|\hat{W}_d\| \right) \text{sgn}(r) \right) \quad (24) \end{aligned}$$

where  $\tilde{W}_d \in \mathbb{R}$  is the learning estimation error defined as  $\tilde{W}_d = \sum_{i \in \mathcal{A}} \tilde{W}_{d,i} \triangleq \sum_{i \in \mathcal{A}} (W_{d,i} - \hat{W}_{d,i}) = W_d - \hat{W}_d$ . Based on the periodicity and boundedness of  $W_d$ ,  $W_d(t) = \sum_{i \in \mathcal{A}} \text{sat}_{\beta_i}(W_{d,i}(t)) = \sum_{i \in \mathcal{A}} \text{sat}_{\beta_i}(W_{d,i}(t - T))$ . Hence, by exploiting (21), the following expression can be developed for  $\tilde{W}_d$ :

$$\begin{aligned} \tilde{W}_d &= \sum_{i \in \mathcal{A}} \tilde{W}_{d,i} \\ &= \sum_{i \in \mathcal{A}} \text{sat}_{\beta_i}(W_{d,i}(t - T)) \\ &\quad - \sum_{m \in \mathcal{M}} \sigma_m \left( \text{sat}_{\beta_m}(\hat{W}_{d,m}(t - T)) + k_{L,m} r \right) \\ &\quad - \sigma_e \left( \text{sat}_{\beta_e}(\hat{W}_{d,e}(t - T)) + k_{L,e} r \right). \quad (25) \end{aligned}$$

To incorporate the repetitive learning error term in the subsequent stability analysis, an auxiliary function  $Q : \mathbb{R}_{\geq t_0} \rightarrow \mathbb{R}$  is defined as

$$Q \triangleq \sum_{i \in \mathcal{A}} \frac{1}{2k_{L,i}} \int_{t-T}^t \left( \text{sat}_{\beta_i}(W_{d,i}(\varphi)) - \text{sat}_{\beta_i}(\hat{W}_{d,i}(\varphi)) \right)^2 d\varphi. \quad (26)$$

#### V. STABILITY ANALYSIS

*Theorem 1:* The controller in (20) with the repetitive learning law in (21) ensures global asymptotic cadence tracking provided the control gains are selected to satisfy the following sufficient conditions:

$$\alpha_1, \alpha_2 > \frac{1}{2}, k_2 > \frac{\Theta}{c_b}, k_3 > \frac{1}{c_b}, k_4 > \frac{1 + c_B}{c_b}. \quad (27)$$

<sup>2</sup>The control objective is quantified using the second time derivative of  $e_1$ .

*Proof:* Let  $V_1 : \mathbb{R}^4 \times \mathbb{R}_{\geq t_0} \rightarrow \mathbb{R}$  be a non-negative, continuously differentiable, function defined as

$$V_1 \triangleq \frac{1}{2}e_1^2 + \frac{1}{2}e_2^2 + \frac{1}{2}Mr^2 + Q. \quad (28)$$

The function in (28) satisfies the following inequalities:

$$\lambda_1 \|y\|^2 \leq V_1(y, t) \leq \lambda_2 \|y\|^2$$

where  $\lambda_1 \triangleq \min([1/2], [1/2]c_m, [1/2k_{L,i}])$ ,  $\lambda_2 \triangleq \max([1/2], [1/2]c_M, [1/2k_{L,i}])$ ,  $\forall i \in \mathcal{A}$  and  $y \triangleq [z^T \sqrt{Q_L}]^T$  where  $Q_L \triangleq \sum_{i \in \mathcal{A}} \int_{t-T}^t (\text{sat}_{\beta_i}(W_{d,i}(\varphi)) - \text{sat}_{\beta_i}(\hat{W}_{d,i}(\varphi)))^2 d\varphi$ . Let  $y(t)$  be a Filippov solution to the differential inclusion  $\dot{y} \in K[h](y)$ , where  $K[\cdot]$  is defined as in [41], and  $h$  is defined by using (10), (11), and (24) as  $h \triangleq [h_1 \ h_2 \ h_3 \ h_4]$ , where  $h_1 \triangleq e_2 - \alpha_1 e_1$ ,  $h_2 \triangleq r - \alpha_2 e_2$ ,  $h_3 \triangleq M^{-1}\{-Vr + \chi + N_d + \tilde{W}_d + \hat{W}_d - e_2 - B_\sigma(\hat{W}_d + k_1 r + (k_2 + k_3 \rho(\|z\|)\|z\| + k_4 \|\hat{W}_d\|) \text{sgn}(r))\}$ ,  $h_4 \triangleq (1/2\sqrt{Q_L}) \sum_{i \in \mathcal{A}} \{(\text{sat}_{\beta_i}(W_{d,i}(t)) - \text{sat}_{\beta_i}(\hat{W}_{d,i}(t)))^2 - (\text{sat}_{\beta_i}(W_{d,i}(t-T)) - \text{sat}_{\beta_i}(\hat{W}_{d,i}(t-T)))^2\}$ . The control input in (20) includes the signum function and the discontinuous lumped control effectiveness  $B_\sigma$ ; hence, the time derivative of (28) exists almost everywhere (a.e.), i.e., for almost all  $t$ . Based on [39, Lemma 1], the time derivative of (28),  $\dot{V}_1(y(t), t) \stackrel{\text{a.e.}}{=} \dot{V}_1(y(t), t)$ , where  $\dot{V}_1$  is the generalized time derivative of (28) along the Filippov trajectories of  $\dot{y} = h(y)$  is defined as  $\dot{V}_1 \triangleq \bigcap_{\xi \in \partial V_1} \xi^T K[\dot{e}_1 \ \dot{e}_2 \ \dot{r} \ (\dot{Q}_L/2\sqrt{Q_L}) \ 1]^T (e_1, e_2, r, 2\sqrt{Q_L}, t)$ , where  $\partial V_1(y, t)$  is the generalized gradient of  $V_1$  at  $(y, t)$  defined as  $\partial V_1(y, t) = \overline{\text{co}}\{\lim \nabla V_1(y, t) | (y_i, t_i) \rightarrow (y, t), (y_i, t_i) \notin \Omega_{V_1}\}$ , where  $\Omega_{V_1}$  is the set of measure zero where the gradient of  $V_1$  is not defined and  $\overline{\text{co}}$  denotes the convex closure [39], [42]. Since  $V_1(y, t)$  is continuously differentiable in  $y$ ,  $\partial V_1 = \{\nabla V_1\}$ , thus

$$\dot{V}_1 \stackrel{\text{a.e.}}{\subset} [e_1, e_2, Mr, \sum_{i \in \mathcal{A}} \left( \frac{1}{2k_{L,i}} \right) 2\sqrt{Q_L}, \frac{1}{2}Mr^2] K \begin{bmatrix} \dot{e}_1 \\ \dot{e}_2 \\ \dot{r} \\ \frac{\dot{Q}_L}{2\sqrt{Q_L}} \\ 1 \end{bmatrix}.$$

Therefore, after substituting for (10), (11), and (24), and using Property 5, the generalized time derivative of (28) can be expressed as

$$\begin{aligned} \dot{V}_1 \stackrel{\text{a.e.}}{\subset} & e_1 e_2 - \alpha_1 e_1^2 - \alpha_2 e_2^2 \\ & + r \left( \tilde{W}_d + \hat{W}_d + \chi + N_d + K[B_\sigma] \hat{W}_d - K[B_\sigma] k_1 r \right. \\ & \quad \left. - K[B_\sigma \text{sgn}(r)] \left( k_2 + k_3 \rho(\|z\|)\|z\| + k_4 \|\hat{W}_d\| \right) \right) \\ & + \sum_{i \in \mathcal{A}} \frac{1}{2k_{L,i}} \left( \text{sat}_{\beta_i}(W_{d,i}(t)) - \text{sat}_{\beta_i}(\hat{W}_{d,i}(t)) \right)^2 \\ & - \sum_{i \in \mathcal{A}} \frac{1}{2k_{L,i}} \left( \text{sat}_{\beta_i}(W_{d,i}(t-T)) - \text{sat}_{\beta_i}(\hat{W}_{d,i}(t-T)) \right)^2 \end{aligned} \quad (29)$$

where  $K[\text{sgn}(r)] = \text{SGN}(r)$  and  $K[B_\sigma] \subset [c_b, c_B]$ . Substituting for (16), (17), and (25), and using Property 6

and Young's inequality, an upper bound for (29) can be developed as

$$\begin{aligned} \dot{V}_1 \stackrel{\text{a.e.}}{\leq} & - \left( \alpha_1 - \frac{1}{2} \right) e_1^2 - \left( \alpha_2 - \frac{1}{2} \right) e_2^2 - k_1 c_b r^2 \\ & - (k_2 c_b - \Theta) |r| - (k_3 c_b - 1) \rho(\|z\|) \|z\| |r| \\ & - (k_4 c_b - 1 - c_B) \|\hat{W}_d\| |r| \\ & + \sum_{i \in \mathcal{A}} \frac{1}{2k_{L,i}} \left( \text{sat}_{\beta_i}(W_{d,i}(t)) - \text{sat}_{\beta_i}(\hat{W}_{d,i}(t)) \right)^2 \\ & + \tilde{W}_d r - \sum_{i \in \mathcal{A}} \frac{1}{2k_{L,i}} (\tilde{W}_{d,i} + k_{L,i} r)^2. \end{aligned} \quad (30)$$

By employing the following property:

$$\left( W_{d,i}(t) - \hat{W}_{d,i}(t) \right)^2 \geq \left( \text{sat}_{\beta_i}(W_{d,i}(t)) - \text{sat}_{\beta_i}(\hat{W}_{d,i}(t)) \right)^2$$

as proven in [25, Appendix I], and canceling terms, (30) can be rewritten as

$$\begin{aligned} \dot{V}_1 \stackrel{\text{a.e.}}{\leq} & - \left( \alpha_1 - \frac{1}{2} \right) e_1^2 - \left( \alpha_2 - \frac{1}{2} \right) e_2^2 \\ & - \left( k_1 c_b + \frac{k_{L,\min}}{2} \right) r^2 - (k_2 c_b - \Theta) |r| \\ & - (k_3 c_b \rho(\|z\|) \|z\| - \rho(\|z\|) \|z\|) |r| \\ & - (k_4 c_b - 1 - c_B) \|\hat{W}_d\| |r| \end{aligned} \quad (31)$$

where the minimum learning gain  $k_{L,\min} \in \mathbb{R}_{>0}$  is defined as  $k_{L,\min} \triangleq \min\{k_{L,i}\}$ ,  $\forall i \in \mathcal{A}$ . Provided the gain conditions in (27) are satisfied, the inequality in (31) can be further upper bounded as

$$\dot{V}_1 \stackrel{\text{a.e.}}{\leq} -\delta \|z\|^2 \quad (32)$$

where  $\delta \in \mathbb{R}$  is defined as

$$\delta \triangleq \min \left\{ \left( \alpha_1 - \frac{1}{2} \right), \left( \alpha_2 - \frac{1}{2} \right), \left( k_1 c_b + \frac{k_{L,\min}}{2} \right) \right\}.$$

By invoking [39, Corollary 2],  $|e_1|, |e_2|, |r| \rightarrow 0$  as  $t \rightarrow \infty$ . Since  $V_1 > 0$  and  $\dot{V}_1 \stackrel{\text{a.e.}}{\leq} 0$ ,  $V_1 \in \mathcal{L}_\infty$ , hence,  $e_1, e_2, r, Q_L \in \mathcal{L}_\infty$ . From (21),  $\hat{W}_d \in \mathcal{L}_\infty$ , which along with the fact that  $W_d \in \mathcal{L}_\infty$  from (19), implies that  $\tilde{W}_d \in \mathcal{L}_\infty$ . Then from (20),  $v \in \mathcal{L}_\infty$ , and from (5) and (6),  $u_m, u_e \in \mathcal{L}_\infty$ , which implies  $\tau_a, \tau_e \in \mathcal{L}_\infty$ . Since  $e_1, e_2, r \in \mathcal{L}_\infty$ , then  $\dot{e}_1, \dot{e}_2 \in \mathcal{L}_\infty$  from (10) and (11), and hence,  $q, \dot{q} \in \mathcal{L}_\infty$ , which implies  $\ddot{q} \in \mathcal{L}_\infty$  from (7). ■

## VI. EXPERIMENTS

The cadence controller developed in (20) with the distributed repetitive learning-based feedforward control in (21) was implemented in experiments with able-bodied individuals and people with NCs. The switched control input was commanded as stimulation intensities  $u_m$  in (5) to activate the right and left quadriceps ( $RQ, LQ$ ), hamstrings ( $RH, LH$ ), and gluteal ( $RG, LG$ ) muscle groups and as current  $u_e$  in (6) to the electric motor.

TABLE I  
DEMOGRAPHICS OF PARTICIPANTS WITH AN NC

Subject	Age	Sex	Injury	Months Since Injury
A	28	F	SCI T8-T9	135
B	25	M	SB L5-S1	Since Birth
C	28	F	MS	96
D	32	M	SCI C5-C7, T12	76
E	48	F	Hemorrhagic Stroke	16

### A. Subjects

Seven able-bodied individuals (five males and two females) with ages ranging between 22 and 43 years old participated in the FES-cycling protocol at the University of Florida. Participants with NCs (two males and three females) were either recruited through the UF Health Integrated Data Repository (UF Consent2Share project) and completed the FES-cycling protocol at the University of Florida or were enrolled at Brooks Rehabilitation in Jacksonville, FL, USA. Demographics of the participants with NCs are listed in Table I. The participants with NCs were medically stable and met the inclusion criteria. Prior to participation, written informed consent was obtained from all participants, as approved by the Institutional Review Board at the University of Florida. The participants with NCs self-reported their motor function and mobility status. Both able-bodied participants and people with NCs were instructed to avoid voluntarily contributing. The able-bodied individuals were not informed of the cycling objective of the protocol. The neurologically impaired individuals were informed of the cycling cadence objective, but no feedback regarding the performance was provided throughout the experiments. Subject A is a paraplegic due to SCI (T8-T9 complete) with previous limited experience with FES technologies. Subject A used a wheelchair full-time for mobility. Subject B is a participant with Spina Bifida (SB) (L5-S1 level) and Arnold Chiari malformation. Subject B used a wheelchair part-time for mobility and a walker for ambulation at home. Subject C is a participant with relapsing remitting MS and used a single point cane for ambulation. Subject C presented tremor in her lower extremities during ambulation. Subject D is a quadriplegic due to an SCI (C5-C7, and incomplete T12) with previous experience with upper- and lower-limb cycling and used an electric-powered wheelchair for mobility. Subject E is a post-hemorrhagic stroke participant with left side impairment and minor loss of sensory perception. Subject E used a single point cane for ambulation and had an ankle foot orthosis.

### B. Experimental Setup

Testing was performed using a recumbent tricycle (TerraTrike Rover) mounted on an indoor trainer and adapted with orthotic boots. A brushed 24 VDC electric motor was coupled to the drive chain. An optical encoder (U.S. Digital) measured the crank position. The FES-cycling testbed is illustrated in Fig. 1. The controller was implemented using a personal computer (Windows 10 OS) running a real-time target (QUARC 2.5, Quanser) via MATLAB/Simulink 2015b (MathWorks, Inc.) with a sample rate of 500 Hz. The Quanser Q8-USB data acquisition board was used to read the encoder

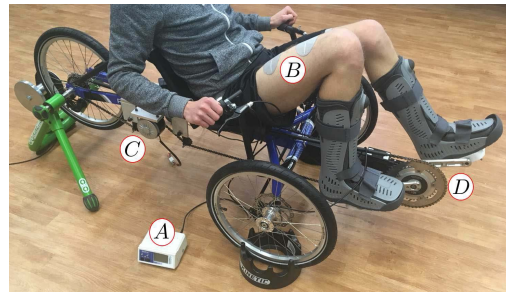


Fig. 1. Motorized FES-cycling test bed. A) Current-controlled electrical stimulator. B) Surface electrodes. C) DC motor. D) Cycle crank fitted with sensors.

and to interface with an analog motor driver and a filter card (Advanced Motion Controls)<sup>3</sup> that commanded the current control to the electric motor. The filter card provided additional inductance to the motor and reduced the electromagnetic interference. A current-controlled 8-channel stimulator (RehaStim, Hasomed GmbH) delivered biphasic, symmetric, and rectangular pulses to the participant's muscle groups. Self-adhesive PALS electrodes (3" by 5")<sup>4</sup> were placed on each muscle group in both extremities according to the electrode's manufacturer manual. For some participants, electrodes (2" by 4") were placed on the gluteal muscle groups based on personal preferences. The stimulation current amplitude was fixed at 90 mA for the quadriceps, 80 mA for the hamstrings, and 70 mA for the gluteal muscle groups. The stimulation frequency was fixed at 60 Hz, and the pulsewidth was computed by  $u_m$  in (5) and (20)–(22) and commanded to the stimulator via serial port communication. Anatomical lengths of the participant's lower extremities were recorded utilizing visible landmarks as in [11]. These measurements were used to determine the stimulation pattern (i.e., the crank angles where the muscle groups were electrically stimulated).

Cadence trials with only the motor being activated were implemented to familiarize the participants with NCs with different operating speeds. Afterward, open-loop stimulation pulse trains were delivered to the participants with NCs to determine the minimum threshold that elicits visible muscle contractions. The experiment duration  $t_d$  was 3 min. The desired cadence trajectory  $\dot{q}_d$  smoothly approached a steady state value of 50 revolutions per minute (RPM) during the time interval,  $t \in [0, t_1]$ ,  $t_1 = 16$  s, during which, only the motor was activated (i.e.,  $\sigma_e = 1$ ,  $q \in \mathcal{Q}_e$  for the whole crank cycle). The cadence trajectory remained constant at 50 RPM for a transition time interval of 10 s,  $t \in [t_1, t_1 + 10]$ , where the regions of the crank cycle for which electrical stimulation was delivered (i.e.,  $q \in \mathcal{Q}_m$ ) increased until it reached a steady state value. After the transition interval, the desired cadence began its periodic trajectory and the stimulation regions remained constant until the end of the experiment (i.e.,  $t \in [t_1 + 10, t_d]$ ).

The periodic crank velocity tracked by the learning controller in (21) had an amplitude of  $50 \pm 5$  RPM and a period

<sup>3</sup>The servo drive and filter card were provided in part by the sponsorship of Advanced Motion Controls.

<sup>4</sup>Surface electrodes for the study were provided compliments of Axelgaard Manufacturing Company, Ltd.

TABLE II

TRACKING RESULTS FOR HEALTHY PARTICIPANTS: AVERAGE CADENCE TRACKING ERROR  $\ddot{e}_1$ , AVERAGE POSITION TRACKING ERROR  $\dot{e}_1$ , CADENCE RMS ERROR (MOVING WINDOW OF 12 s), AND CADENCE PERCENT ERROR REPORTED AS MEAN VALUE  $\pm$  STANDARD DEVIATION

Subject	$\ddot{e}_1$ (RPM)	$\dot{e}_1$ (deg)	RMS (RPM)	% Error
S1	0.04 $\pm$ 3.57	0.01 $\pm$ 3.28	3.57 $\pm$ 0.30	0.06 $\pm$ 7.26
S2	0.05 $\pm$ 3.76	0.00 $\pm$ 4.35	3.75 $\pm$ 0.27	0.08 $\pm$ 7.61
S3	0.07 $\pm$ 3.57	0.25 $\pm$ 11.65	3.55 $\pm$ 0.39	0.08 $\pm$ 7.22
S4	0.04 $\pm$ 4.04	0.02 $\pm$ 9.24	4.01 $\pm$ 0.55	0.05 $\pm$ 8.26
S5	0.07 $\pm$ 3.22	0.02 $\pm$ 3.84	3.23 $\pm$ 0.20	0.12 $\pm$ 6.52
S6	0.06 $\pm$ 3.44	0.02 $\pm$ 3.24	3.43 $\pm$ 0.45	0.11 $\pm$ 7.04
S7	0.00 $\pm$ 3.63	0.76 $\pm$ 14.90	3.57 $\pm$ 0.64	0.01 $\pm$ 7.40
Mean	0.03 $\pm$ 3.61	0.15 $\pm$ 8.43	3.58 $\pm$ 0.43	0.07 $\pm$ 7.35

TABLE III

TRACKING RESULTS FOR PARTICIPANTS WITH NCs: AVERAGE CADENCE TRACKING ERROR  $\ddot{e}_1$ , AVERAGE POSITION TRACKING ERROR  $\dot{e}_1$ , CADENCE RMS ERROR (MOVING WINDOW OF 12 s), AND CADENCE PERCENT ERROR REPORTED AS MEAN VALUE  $\pm$  STANDARD DEVIATION

Subject	$\ddot{e}_1$ (RPM)	$\dot{e}_1$ (deg)	RMS (RPM)	% Error
A	0.04 $\pm$ 3.90	0.02 $\pm$ 6.57	3.89 $\pm$ 0.30	0.05 $\pm$ 7.93
B	0.02 $\pm$ 4.53	0.04 $\pm$ 4.93	4.48 $\pm$ 0.77	0.03 $\pm$ 9.35
C	0.06 $\pm$ 3.89	0.05 $\pm$ 16.40	3.80 $\pm$ 0.81	0.15 $\pm$ 8.00
D	0.02 $\pm$ 5.24	0.88 $\pm$ 33.55	5.07 $\pm$ 1.34	0.21 $\pm$ 10.96
E	0.03 $\pm$ 4.08	0.08 $\pm$ 4.95	4.06 $\pm$ 0.64	0.06 $\pm$ 8.37
Mean	0.03 $\pm$ 4.36	0.21 $\pm$ 17.24	4.26 $\pm$ 0.84	0.1 $\pm$ 8.99

of  $T = 12$  s and was commanded for  $t \in [t_1 + 10, t_d]$ . To facilitate the selection of gains in (5), (6), (20), (22), and (23), separate gains were selected for each muscle group and the electric motor, without loss of generality. The control gains introduced in (5), (6), (10), (11), (20), (22), and (23) were selected as follows<sup>5</sup>:  $k_m \in [0.45, 0.5]$ ,  $k_e \triangleq 10$ ,  $\alpha_1 \in [0.625, 0.75]$ ,  $\alpha_2 \in [1.5, 1.75]$ ,  $k_{1,m} \in [65, 520]$ ,  $k_{2,m} \in [5, 28]$ ,  $k_{3,m} \in [0.01, 0.08]$ ,  $k_{4,m} \in [0.5, 1.5]$ ,  $k_{1,e} \triangleq 1$ ,  $k_{2,e} \triangleq 0.3$ ,  $k_{3,e} \triangleq 0.001$ ,  $k_{4,e} \triangleq 0.001$ ,  $k_{L,m} = [k_{L,RQ}, k_{L,LQ}, k_{L,RH}, k_{L,LH}, k_{L,RG}, k_{L,LG}] \in [[15, 90], [15, 90], [12, 80], [16, 80], [12, 75], [14, 75]]$ , and  $k_{L,e} \in [0.15, 0.18]$ . The muscle control gains were selected based on the performance obtained during a brief pretrial. The gain tuning was motivated to yield consistent performance for all the participants despite the differences in the physical characteristics of the individuals.

### C. Results

The FES-cycling experiments were successfully completed by all the enrolled participants. Table II summarizes the average cadence tracking error  $\ddot{e}_1$ , the average position tracking error  $\dot{e}_1$ , the cadence root-mean-squared (RMS) error, and the cadence percent error (% error) during  $t \in [t_1, t_d]$  seconds for the healthy individuals (S1–S7). Table III reports the results for the participants with NCs (A–E). The cadence RMS error was calculated over a moving time interval window corresponding to the period of the desired trajectory, i.e., 12 s. Fig. 2 shows the switching of the stimulation intensities  $u_m$ , the muscle

<sup>5</sup>The control gains for the experiments were tuned using empirical methods. In contrast to this approach, the control gains could have been adjusted using more methodical approaches to find optimal gains as described in various survey papers on the topic [43], [44].

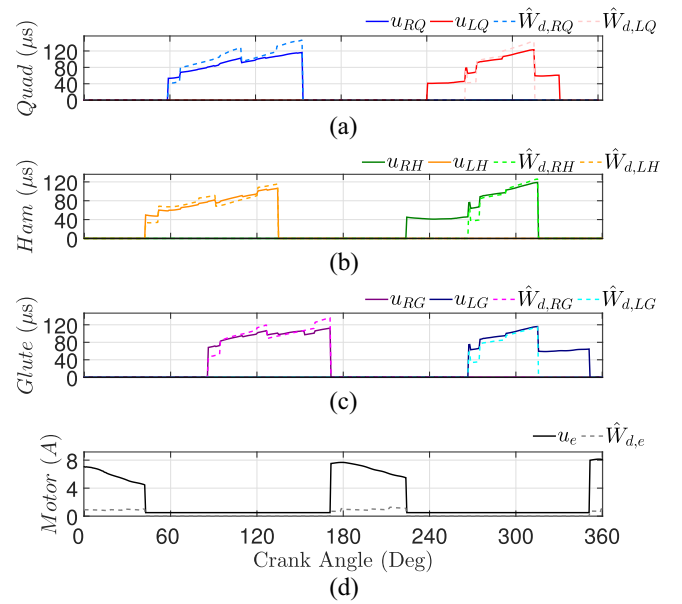


Fig. 2. FES stimulation intensities  $u_m$  (solid lines) and muscle learning feedforward terms  $\hat{W}_{d,m}$  (dashed lines) delivered to the (a) right (R) and left (L) quadriceps, (b) hamstrings, and (c) gluteal muscle groups, and (d) motor current input  $u_e$  (solid line) and motor learning feedforward term  $\hat{W}_{d,e}$  (dashed line) delivered to the electric motor over one crank cycle for Subject S4. This figure illustrates the switching of the control inputs designed in (5) and (6).

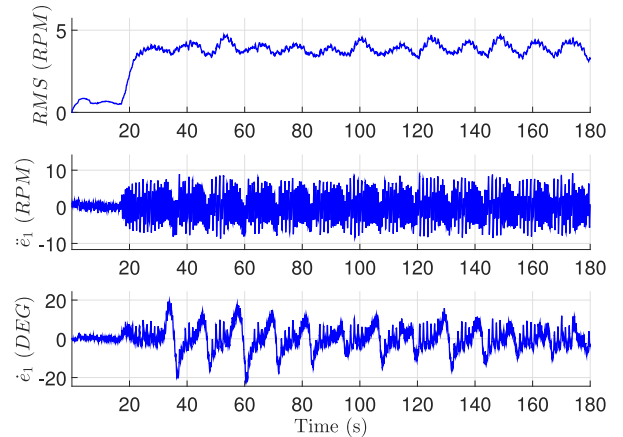


Fig. 3. Tracking performance for Subject A quantified by the cadence RMS error with a moving time interval window of 12 s (the same as the period  $T$  of  $\dot{q}_d$  for  $t \in [t_1 + 10, t_d]$ ) (top), the average cadence tracking error  $\ddot{e}_1$  (middle), and the average position error  $\dot{e}_1$  (bottom).

learning feedforward inputs  $\hat{W}_{d,m}$ , the motor current input  $u_e$ , and the electric motor learning feedforward input  $\hat{W}_{d,e}$  over a single crank cycle for Subject S4 after 2 min of cadence tracking. Fig. 3 shows the cadence tracking performance quantified by the cadence RMS error (top), the cadence tracking error  $\ddot{e}_1$  (middle), and the position tracking error  $\dot{e}_1$  (bottom) of Subject A. Fig. 4 illustrates the stimulation intensities delivered to the muscle groups  $u_m$  and the electric motor current input  $u_e$  for the entire experiment duration for Subject A.

To assess the effect of the distributed feedforward RLC component, two trials with different learning gains were performed for Subject S5 (selected randomly from the healthy individuals). Fig. 5 depicts the distributed muscle and electric

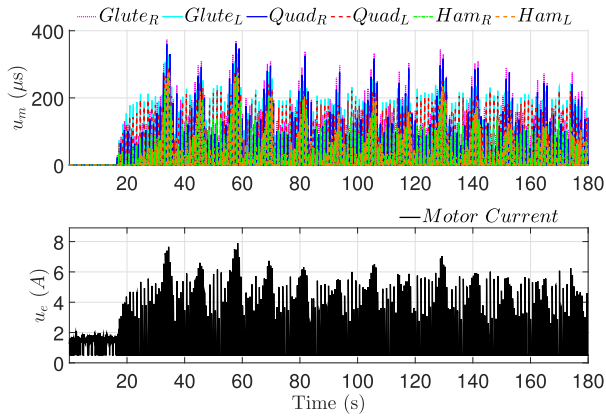


Fig. 4. Stimulation intensity delivered to each muscle group  $u_m$  (top) and the electric motor current input  $u_e$  (bottom) for Subject A.

motor learning feedforward terms (i.e.,  $\hat{W}_{d,m}$  and  $\hat{W}_{d,e}$ ) for the two trials. Fig. 5(a)–(d) illustrates the first trial where the muscle learning gains were set to  $k_{L,m} = [20; 20; 18; 18; 15; 15]$  and  $k_{1,m} = 85$ . Fig. 5(e)–(h) depicts the second trial where the muscle learning gains were doubled compared to the first trial and  $k_{1,m} = 65$ . For both trials, the electric motor learning gain was set to  $k_{L,e} = 0.18$ . Fig. 6 shows the corresponding tracking performance of the two trials quantified by the cadence RMS error and the position tracking error  $\dot{e}_1$ . Fig. 6(a) and (b) corresponds to the first trial and Fig. 6(c) and (d) for the second trial.

Fig. 7 illustrates the muscle and electric motor learning feedforward terms  $\hat{W}_{d,m}$  and  $\hat{W}_{d,e}$  for Subject A (a)–(d) and Subject S3 (e)–(h). The differences in amplitude, symmetry, and duration of the learning feedforward inputs can be contrasted for a participant with a movement disorder (Subject A) and an able-bodied individual (Subject S3).

#### D. Discussion

The experimental results conducted in healthy individuals and participants with NCs demonstrate the feasibility of the controllers developed in (5) and (6) with distributed repetitive learning inputs designed in (22) and (23) to cooperatively track a desired cadence trajectory. The average cadence tracking error  $\dot{e}_1$  is  $0.03 \pm 3.61$  RPM for seven able-bodied individuals and  $0.03 \pm 4.36$  RPM for five participants with NCs. The average position tracking error  $\dot{e}_1$  is  $0.15 \pm 8.43^\circ$  for able-bodied individuals and  $0.21 \pm 17.24^\circ$  for the participants with NCs (see Tables II and III).

The average cadence and position tracking errors are similar to the results reported in the FES-cycling literature such as [10], [11], [38], and [45]. The cadence tracking performance for both healthy and neurologically impaired individuals in this paper is consistent with the cadence performance reported in [10], where a robust approach was employed, and with [45], where an RISE-based approach was implemented, exploiting the stimulation of antagonistic biarticular muscles. The cycling experiments performed in [10] included healthy individuals only and in [45] several able-bodied participants and one subject with Parkinson’s disease. The implementation of

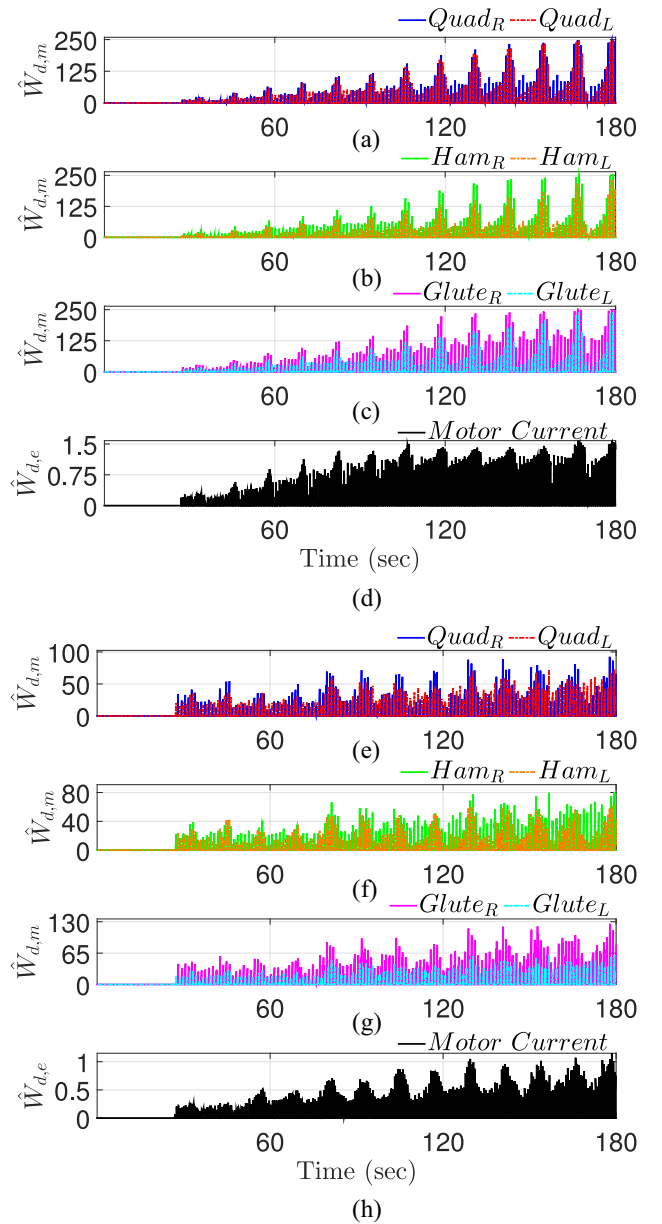


Fig. 5. Effect of modifying muscle learning gains  $k_{L,m}$  on  $\hat{W}_{d,m}$  and  $\hat{W}_{d,e}$  during two different trials for Subject S5. For the first and second trials, the muscle learning feedforward terms  $\hat{W}_{d,m}$  are shown for the (a) and (e) right (R) and left (L) quadriceps, (b) and (f) hamstrings, and (c) and (g) gluteal muscle groups, and the (d) and (h) electric motor learning feedforward term  $\hat{W}_{d,e}$ .

the distributed RLC adds a feedforward term to each of the lower-limb muscle group stimulation intensities and electric motor current based on its past inputs. By the construction of  $r$  in (11), the muscle and electric motor learning feedforward terms have a proportional–integral–derivative form and affect both cadence and position tracking.

The feedforward RLC term has a significant effect in the tracking performance as depicted in the two trials (using different muscle learning gains  $k_{L,m}$ ) for Subject S5 in Fig. 6. The cadence RMS error and position error in Fig. 6(a) and (b), respectively, depict the tracking performance of the first trial. After 100 s, oscillations of both the cadence RMS error

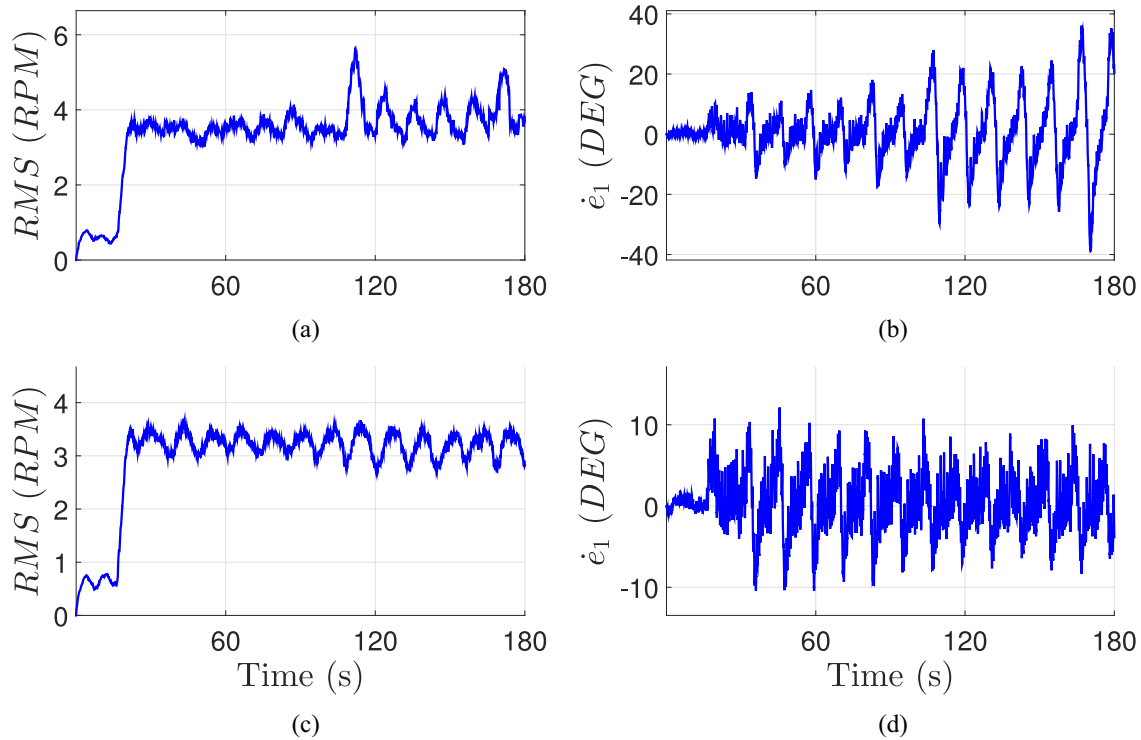


Fig. 6. Tracking performance for Subject S5 during two trials with different muscle learning gains  $k_{L,m}$ . The cadence RMS error is depicted in (a) first trial and (c) second trial. The position tracking error  $\dot{e}_1$  is depicted in (b) first trial and (d) second trial.

[Fig. 6(a)] and position tracking error [Fig. 6(b)] occur due to the high robust gain  $k_{1,m}$  which results in higher stimulation intensities. The muscle learning feedforward terms  $\hat{W}_{d,m}$  in Fig. 5(a)–(c) grew consistently reaching a maximum of  $250 \mu\text{s}$  at the end of the first trial. The first trial resulted in increased stimulation intensities  $u_m$  that induced discomfort, which may potentially result in early experiment termination particularly for participants with greater sensitivity to the stimulation. Also, it is well known that higher stimulation intensities result in increased muscle fatigue which inherently limits the experiment duration due to the rapid decay of muscle force. The cadence tracking percent error during the first trial shown in Fig. 6(a) is  $0.03 \pm 7.52\%$ . Alternatively, the cadence RMS error and position tracking error in Fig. 6(c) and (d), respectively, illustrate a steady tracking performance during the second trial. In the second trial, the muscle learning gains  $k_{L,m}$  were doubled and the gain  $k_{1,m}$  was reduced compared to the first trial. The cadence RMS error in Fig. 6(c) drops below 3 RPM intermittently and never crosses 4 RPM. The position tracking error  $\dot{e}_1$  in Fig. 6(d) decreases in amplitude from period to period. Consistently, the muscle learning feedforward terms  $\hat{W}_{d,m}$  in Fig. 5(e)–(g) illustrate steady learning inputs across all muscle groups reaching maxima of  $90 \mu\text{s}$  for the quadriceps,  $80 \mu\text{s}$  for the hamstrings, and  $100 \mu\text{s}$  for the gluteal muscle groups during the second trial. The cadence tracking percent error during the second trial shown in Fig. 6(c) is  $0.12 \pm 6.52\%$ . As depicted in the second trial, steady stimulation inputs result in smoother cadence tracking and prevents overstimulation of the muscles, potentially enabling longer cycling sessions.

The distributed RLC is able to adapt for participants with NCs. In Fig. 7(a) and (c), the quadriceps and gluteal learning feedforward terms  $\hat{W}_{d,m}$  illustrate high amplitude and asymmetric profiles. These learning inputs may be representative of the lack of neurological motor control and muscle weakness of Subject A (SCI participant). The learning feedforward terms for the right quadriceps ( $\hat{W}_{d,RQ}$ ) and glutes ( $\hat{W}_{d,RG}$ ) had higher magnitudes with mean values of  $82$  and  $89 \mu\text{s}$  than their left counterparts. In Fig. 7 (e)–(h), the muscle and electric motor learning feedforward terms  $\hat{W}_{d,m}$  and  $\hat{W}_{d,e}$  denote steady and more symmetric profiles for Subject S3 (able-bodied participant) with mean magnitudes for all muscle groups between  $40$  and  $50 \mu\text{s}$ . These learning inputs may be representative of the symmetry between the legs and the high muscle strength of the healthy participant.

The percentage of time during which the participants with NCs were actively stimulated suggests an adequate balance between the FES and motorized contributions to maintain the desired cadence. Moreover, stimulation times have a high impact in the rate of muscle fatigue, which affects cycling duration and thus the amount of dose of rehabilitative stimulation. For the SCI participants, Subjects A (paraplegic) and D (quadriplegic), the lack of muscle mass and strength, intermittent spasms, and the lack of neurological motor control resulted in increased stimulation intensities with a mean value across all muscle groups of  $105$  and  $135 \mu\text{s}$ , respectively. The percentage of time during which Subjects A and D were actively stimulated was  $34\%$  and  $31\%$ , respectively, to achieve a balance between the muscle's contributions and the motorized assistance. Subject B, a participant with SB,

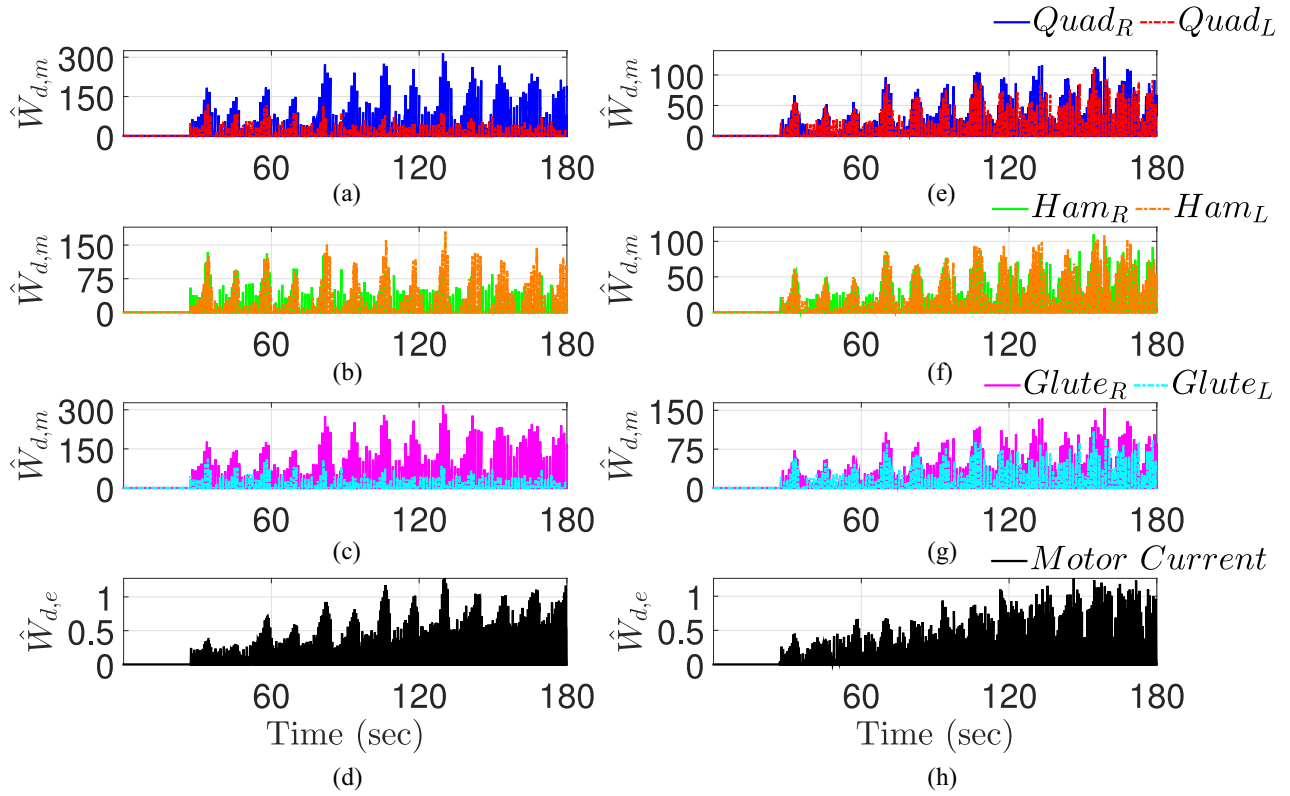


Fig. 7. Muscle learning feedforward terms  $\hat{W}_{d,m}$  for the (a) and (e) right (R) and left (L) quadriceps, (b) and (f) hamstrings, and (c) and (g) gluteal muscle groups, and (d) and (h) electric motor learning feedforward term  $\hat{W}_{d,e}$  for Subject A (impaired), (left column) and Subject S3 (able-bodied individual), (right column).

evoked visible active contractions with 30% of the stimulation intensities required for the SCI participants. The percentage of time during which Subject B was actively stimulated was 32%. Subject C, a participant with MS, needed 25% of the stimulation intensities required for the SCI subjects. Subject C was actively stimulated 45% of the time. Subject E, a post-stroke participant, had residual motor control on her left affected side and full neurological motor control in her contralateral side; however, the subject was asked to not contribute voluntarily during the cadence experiments. Subject E was actively stimulated for 46% of the time with 20% of the stimulation intensities delivered to the SCI participants. Future experiments in a longitudinal study can help to elucidate the clinical significance of longer stimulation times in people with different conditions.

The stability analysis ensures asymptotic tracking; however there are factors during experiments such as muscle fatigue, disturbances in the cycle, and electromechanical delay, which degrade the tracking performance. Nevertheless, the results show that by switching the control effort between the stimulation intensities delivered to the six muscle groups and the electric motor, desirable cadence and position tracking was achieved. Clinical trials with a larger population of participants with NCs are required to investigate the long-term impact of the control methodology developed in this paper. In [46], an FES-cycling study with 25 SCI participants found important gains in neurological, motor, and sensory function and increased muscle volume and strength during

29.1 months. A cycling protocol that adopts the distributed repetitive learning approach for power tracking to monitor the torque contribution of the muscles may lead to a more suitable rehabilitation approach like in strength training.

## VII. CONCLUSION

A nonlinear controller that switches among lower-limb muscles and an electric motor with distributed learning feedforward inputs was designed to yield global asymptotic cadence tracking. The switched muscle and electric motor distributed learning compensates for the periodic dynamics of the desired cadence trajectory. The robust feedback terms in the switched controller aid in rejecting disturbances present in the motorized cycle-rider system. The controller is implemented using a nonlinear model with parametric uncertainties and without the need to perform any identification procedures despite the heterogeneity of conditions across participants. Global asymptotic tracking was achieved with the aid of a corollary to the LaSalle–Yoshizawa theorem for nonsmooth systems.

The distributed repetitive learning switched controller was tested in experiments with seven able-bodied individuals and five participants with NCs, such as SCI, SB, MS, and post-stroke. For the healthy control group and for the neurologically impaired population, a mean RMS (computed over a time window equal to the period  $T = 12$  s) cadence error of  $3.58 \pm 0.43$  RPM ( $0.06 \pm 7.35\%$  average error) and  $4.26 \pm 0.84$  RPM ( $0.1 \pm 8.99\%$  average error) was obtained, respectively.

The results obtained in people with NCs demonstrate the ability of the switched controller to yield consistent repetitive cadence despite lower-limb asymmetries, muscle spasticity, muscle atrophy, tremor, muscle weakness, hypersensitivity, and absence of neurological motor control.

Long-term clinical trials with a larger and broader population, including people with Parkinson's disease, traumatic brain injury, and cerebral palsy are needed to expand the findings of this paper. For future extensions, the distributed learning control technique can be applied for different tracking objectives in FES-based exercises such as power control (i.e., track a desired torque output), which may be more suitable for intense strength training for certain participants with NCs. Furthermore, a cycling protocol where participants with residual neurological motor control can voluntarily contribute to the pedaling may be desirable to test the distributed learning method.

## REFERENCES

- [1] C. A. Rouse, V. H. Duenas, C. Cousin, A. Parikh, and W. E. Dixon, "A switched systems approach based on changing muscle geometry of the biceps brachii during functional electrical stimulation," *IEEE Control Syst. Lett.*, vol. 2, no. 1, pp. 73–78, Jan. 2018.
- [2] B. Lew, N. Alavi, B. K. Randhawa, and C. Menon, "An exploratory investigation on the use of closed-loop electrical stimulation to assist individuals with stroke to perform fine movements with their hemiparetic arm," *Front. Bioeng. Biotechnol.*, vol. 4, p. 20, Mar. 2016.
- [3] J. McCabe, M. Monkiewicz, J. Holcomb, S. Pundik, and J. J. Daly, "Comparison of robotics, functional electrical stimulation, and motor learning methods for treatment of persistent upper extremity dysfunction after stroke: A randomized controlled trial," *Archives Phys. Med. Rehabil.*, vol. 96, no. 6, pp. 981–990, 2015.
- [4] R. J. Downey, T.-H. Cheng, M. J. Bellman, and W. E. Dixon, "Switched tracking control of the lower limb during asynchronous neuromuscular electrical stimulation: Theory and experiments," *IEEE Trans. Cybern.*, vol. 47, no. 5, pp. 1251–1262, May 2017.
- [5] T.-H. Cheng *et al.*, "Identification-based closed-loop NMES limb tracking with amplitude-modulated control input," *IEEE Trans. Cybern.*, vol. 46, no. 7, pp. 1679–1690, Jul. 2016.
- [6] Q. Wang, N. Sharma, M. Johnson, C. M. Gregory, and W. E. Dixon, "Adaptive inverse optimal neuromuscular electrical stimulation," *IEEE Trans. Cybern.*, vol. 43, no. 6, pp. 1710–1718, Dec. 2013.
- [7] K. H. Ha, S. A. Murray, and M. Goldfarb, "An approach for the cooperative control of FES with a powered exoskeleton during level walking for persons with paraplegia," *IEEE Trans. Neural Syst. Rehabil. Eng.*, vol. 24, no. 4, pp. 455–466, Apr. 2016.
- [8] N. A. Alibejji, N. A. Kirsch, and N. Sharma, "A muscle synergy-inspired adaptive control scheme for a hybrid walking neuroprosthesis," *Front. Bioeng. Biotechnol.*, vol. 3, no. 203, pp. 1–13, Dec. 2015.
- [9] N. Alibejji, N. Kirsch, and N. Sharma, "An adaptive low-dimensional control to compensate for actuator redundancy and FES-induced muscle fatigue in a hybrid neuroprosthesis," *Control Eng. Pract.*, vol. 59, pp. 204–219, Feb. 2017.
- [10] M. J. Bellman, R. J. Downey, A. Parikh, and W. E. Dixon, "Automatic control of cycling induced by functional electrical stimulation with electric motor assistance," *IEEE Trans. Autom. Sci. Eng.*, vol. 14, no. 2, pp. 1225–1234, Apr. 2017.
- [11] M. J. Bellman, T. H. Cheng, R. J. Downey, C. J. Hass, and W. E. Dixon, "Switched control of cadence during stationary cycling induced by functional electrical stimulation," *IEEE Trans. Neural Syst. Rehabil. Eng.*, vol. 24, no. 12, pp. 1373–1383, Dec. 2016.
- [12] M. J. Bellman, T.-H. Cheng, R. J. Downey, and W. E. Dixon, "Stationary cycling induced by switched functional electrical stimulation control," in *Proc. Amer. Control Conf.*, 2014, pp. 4802–4809.
- [13] M. J. Bellman, T.-H. Cheng, R. J. Downey, and W. E. Dixon, "Cadence control of stationary cycling induced by switched functional electrical stimulation control," in *Proc. IEEE Conf. Decis. Control*, 2014, pp. 6260–6265.
- [14] C.-S. Kim *et al.*, "Stimulation pattern-free control of FES cycling: Simulation study," *IEEE Trans. Syst., Man, Cybern. C, Appl. Rev.*, vol. 38, no. 1, pp. 125–134, Jan. 2008.
- [15] K. T. Ragnarsson, "Functional electrical stimulation after spinal cord injury: Current use, therapeutic effects and future directions," *Spinal Cord*, vol. 46, no. 4, pp. 255–274, 2008.
- [16] P. Bauer, C. Krewer, S. Golaszewski, E. Koenig, and F. Müller, "Functional electrical stimulation–assisted active cycling—Therapeutic effects in patients with hemiparesis from 7 days to 6 months after stroke: A randomized controlled pilot study," *Archives Phys. Med. Rehabil.*, vol. 96, no. 2, pp. 188–196, 2015.
- [17] D. J. Reinkensmeyer, J. L. Emken, and S. C. Cramer, "Robotics, motor learning, and neurologic recovery," *Annu. Rev. Biomed. Eng.*, vol. 6, no. 1, pp. 497–525, 2004.
- [18] L. Marchal-Crespo and D. J. Reinkensmeyer, "Review of control strategies for robotic movement training after neurologic injury," *J. Neuroeng. Rehabil.*, vol. 6, no. 1, p. 20, 2009.
- [19] O. Raineteau and M. E. Schwab, "Plasticity of motor systems after incomplete spinal cord injury," *Nat. Rev. Neurosci.*, vol. 2, no. 4, pp. 263–273, 2001.
- [20] L. L. Cai *et al.*, "Implications of assist-as-needed robotic step training after a complete spinal cord injury on intrinsic strategies of motor learning," *J. Neurosci.*, vol. 26, no. 41, pp. 10564–10568, 2006.
- [21] D. A. Bristow, M. Tharayil, and A. G. Alleyne, "A survey of iterative learning control: A learning-based method for high-performance tracking control," *IEEE Control Syst. Mag.*, vol. 26, no. 3, pp. 96–114, Jun. 2006.
- [22] H.-S. Ahn, Y. Chen, and K. L. Moore, "Iterative learning control: Brief survey and categorization," *IEEE Trans. Syst., Man, Cybern. C, Appl. Rev.*, vol. 37, no. 6, pp. 1099–1121, Nov. 2007.
- [23] Y. Wang, F. Gao, and F. J. Doyle, "Survey on iterative learning control, repetitive control, and run-to-run control," *J. Process Control*, vol. 19, no. 10, pp. 1589–1600, Dec. 2009.
- [24] C. T. Freeman, E. Rogers, J. H. Burridge, A.-M. Hughes, and K. L. Meadmore, *Iterative Learning Control for Electrical Stimulation and Stroke Rehabilitation* (Control, Automation and Robotics), 1st ed. London, U.K.: Springer-Verlag, 2015. [Online]. Available: <https://www.springer.com/us/book/9781447167259>
- [25] W. E. Dixon, E. Zergeroglu, D. M. Dawson, and B. T. Costic, "Repetitive learning control: A Lyapunov-based approach," *IEEE Trans. Syst., Man, Cybern. B, Cybern.*, vol. 32, no. 4, pp. 538–545, Aug. 2002.
- [26] M. Sun, S. S. Ge, and I. M. Y. Mareels, "Adaptive repetitive learning control of robotic manipulators without the requirement for initial repositioning," *IEEE Trans. Robot.*, vol. 22, no. 3, pp. 563–568, Jun. 2006.
- [27] W. Messner, R. Horowitz, W.-W. Kao, and M. Boals, "A new adaptive learning rule," *IEEE Trans. Autom. Control*, vol. 36, no. 2, pp. 188–197, Feb. 1991.
- [28] J.-X. Xu and J. Xu, "On iterative learning from different tracking tasks in the presence of time-varying uncertainties," *IEEE Trans. Syst., Man, Cybern. B, Cybern.*, vol. 34, no. 1, pp. 589–597, Feb. 2004.
- [29] C. T. Freeman, E. Rogers, A.-M. Hughes, J. H. Burridge, and K. L. Meadmore, "Iterative learning control in health care: Electrical stimulation and robotic-assisted upper-limb stroke rehabilitation," *IEEE Control Syst. Mag.*, vol. 32, no. 1, pp. 18–43, Feb. 2012.
- [30] P. Sampson *et al.*, "Using functional electrical stimulation mediated by iterative learning control and robotics to improve arm movement for people with multiple sclerosis," *IEEE Trans. Neural Syst. Rehabil. Eng.*, vol. 24, no. 2, pp. 235–248, Feb. 2016.
- [31] T. Seel, C. Werner, J. Raisch, and T. Schauer, "Iterative learning control of a drop foot neuroprosthesis—Generating physiological foot motion in paretic gait by automatic feedback control," *Control Eng. Pract.*, vol. 48, pp. 87–97, Mar. 2016.
- [32] X. Zhao, Y. Chu, J. Han, and Z. Zhang, "SSVEP-based brain–computer interface controlled functional electrical stimulation system for upper extremity rehabilitation," *IEEE Trans. Syst., Man, Cybern., Syst.*, vol. 46, no. 7, pp. 947–956, Jul. 2016.
- [33] E. H. Copur, C. T. Freeman, B. Chu, and D. S. Laila, "Repetitive control of electrical stimulation for tremor suppression," *IEEE Trans. Control Syst. Technol.*, to be published. [Online]. Available: <https://ieeexplore.ieee.org/document/8119729>, doi: 10.1109/TCST.2017.2771327.
- [34] A. Hock and A. P. Schoellig, "Distributed iterative learning control for a team of quadrotors," in *Proc. IEEE Conf. Decis. Control*, Dec. 2016, pp. 4640–4646.

- [35] J. Li, D. W. C. Ho, and J. Li, "Distributed adaptive repetitive consensus control framework for uncertain nonlinear leader–follower multi-agent systems," *J. Frankl. Inst.*, vol. 352, no. 11, pp. 5342–5360, Nov. 2015.
- [36] X. Bu, Q. Yu, Z. Hou, and W. Qian, "Model free adaptive iterative learning consensus tracking control for a class of nonlinear multiagent systems," *IEEE Trans. Syst., Man, Cybern., Syst.*, to be published. [Online]. Available: <https://ieeexplore.ieee.org/abstract/document/8016381>, doi: [10.1109/TSMC.2017.2734799](https://doi.org/10.1109/TSMC.2017.2734799).
- [37] D. Meng and K. L. Moore, "Learning to cooperate: Networks of formation agents with switching topologies," *Automatica*, vol. 64, pp. 278–293, Feb. 2016.
- [38] K. J. Hunt *et al.*, "Control strategies for integration of electric motor assist and functional electrical stimulation in paraplegic cycling: Utility for exercise testing and mobile cycling," *IEEE Trans. Neural Syst. Rehabil. Eng.*, vol. 12, no. 1, pp. 89–101, Mar. 2004.
- [39] N. Fischer, R. Kamalapurkar, and W. E. Dixon, "LaSalle–Yoshizawa corollaries for nonsmooth systems," *IEEE Trans. Autom. Control*, vol. 58, no. 9, pp. 2333–2338, Sep. 2013.
- [40] W. E. Dixon, A. Behal, D. M. Dawson, and S. Nagarkatti, *Nonlinear Control of Engineering Systems: A Lyapunov-Based Approach*. Boston, MA, USA: Birkhäuser, 2003.
- [41] A. F. Filippov, "Differential equations with discontinuous right-hand side," in *Fifteen Papers on Differential Equations* (American Mathematical Society Translations), vol. 42. Providence, RI, USA: Amer. Math. Soc., 1964, pp. 199–231.
- [42] F. H. Clarke, *Optimization and Nonsmooth Analysis*. Reading, MA, USA: Addison-Wesley, 1983.
- [43] N. J. Killingsworth and M. Krstic, "PID tuning using extremum seeking: Online, model-free performance optimization," *IEEE Control Syst. Mag.*, vol. 26, no. 1, pp. 70–79, Feb. 2006.
- [44] K. J. Åström, T. Hägglund, C. C. Hang, and W. K. Ho, "Automatic tuning and adaptation for PID controllers—A survey," *Control Eng. Pract.*, vol. 1, no. 4, pp. 669–714, 1993.
- [45] H. Kawai, M. J. Bellman, R. J. Downey, and W. E. Dixon, "Closed-loop position and cadence tracking control for FES-cycling exploiting pedal force direction with antagonistic biarticular muscles," *IEEE Trans. Control Syst. Technol.*, to be published, [Online]. Available: <https://ieeexplore.ieee.org/document/8168400>, doi: [10.1109/TCST.2017.2771727](https://doi.org/10.1109/TCST.2017.2771727).
- [46] C. L. Sadowsky *et al.*, "Lower extremity functional electrical stimulation cycling promotes physical and functional recovery in chronic spinal cord injury," *J. Spinal Cord Med.*, vol. 36, no. 6, pp. 623–631, 2013.

**Victor H. Duenas**, photograph and biography not available at the time of publication.

**Christian A. Cousin**, photograph and biography not available at the time of publication.

**Courtney Rouse**, photograph and biography not available at the time of publication.

**Emily J. Fox**, photograph and biography not available at the time of publication.

**Warren E. Dixon**, photograph and biography not available at the time of publication.